

Structure and Property Characterization of Low-k Dielectric Porous Thin Films

BARRY J. BAUER, ERIC K. LIN, HAE-JEONG LEE,
HOWARD WANG, and WEN-LI WU

National Institute of Standards and Technology, Polymers Division, Electronics Materials Group, 100 Bureau Drive, Stop 8541, Gaithersburg, MD 20899-8541, USA

A novel methodology is developed that uses a combination of high energy ion scattering, x-ray reflectivity, and small angle neutron scattering to characterize the structure and properties of porous thin films. Ion scattering is used to determine the elemental composition of the film for absolute intensity calibration of the x-ray and neutron scattering techniques. X-ray reflectivity is used to measure the average electron density and film thickness. Small angle neutron scattering is used to determine the pore size, structure, and connectivity. Combining information from all three techniques, the film porosity and matrix material density can be uniquely determined.

Key words: Porous thin film, x-ray reflectivity, small-angle neutron scattering, porosity, ion scattering, low-k dielectric material

INTRODUCTION

Low-k dielectric materials have been identified by the microelectronics industry as a critical factor to enable deep submicron technology for improved performance of integrated circuits. Nanoporous materials have become an important class of low dielectric constant (low-k) materials because the incorporation of voids reduces the dielectric constant of the film by lowering the overall material density.¹ Many strategies have been developed to incorporate pores into thin films including the thermal decomposition of a porogen within a bulk material, sol-gel processing methods, and surfactant-templated pore development. Unlike traditional homogeneous dielectric materials, the two phase structure of the porous network affects properties needed for their integration into current fabrication lines. It is critical to be able to measure the on-wafer structural properties of these porous thin films to understand and to predict correlations between processing conditions and the resulting physical properties. Currently, there are few experimental techniques able to measure the porosity of thin films as prepared on a silicon substrate.²⁻⁴

In this work, we provide unique on-wafer measurements of physical and structural properties of porous

thin films important in the field of low-k materials. More specifically, we have developed a novel methodology to measure the average pore size, pore connectivity, film thickness, matrix material density, coefficient of thermal expansion, moisture uptake, and film elemental composition.⁴⁻⁶ The methodology we developed is a combination of small angle neutron scattering, specular x-ray reflectivity, and ion scattering techniques to determine important structural information about the film. These measurements are performed directly on films prepared and supported on silicon substrates.

EXPERIMENTAL

High Energy Ion Scattering

The elemental composition of the films are determined by Rutherford backscattering spectroscopy (RBS) for silicon, carbon, and oxygen and forward recoil elastic spectroscopy (FRES) for hydrogen. In both techniques, a beam of high energy ions is directed toward the sample surface. The number of scattered particles is counted as a function of their energy.⁷ The elemental composition of the film can be determined because the scattered energy is dependent upon the mass of each elemental species. Fits are performed on the scattered peaks to compute the relative fraction of each element. The measurements

(Received October 19, 2000; accepted November 25, 2000)

were performed at the Surface and Thin Film Analysis Facility at the University of Pennsylvania.⁸

Specular X-ray Reflectivity

The x-ray reflectivity experiments were performed at grazing incident angles on a modified θ - 2θ x-ray diffractometer at the specular condition with the incident angle equal to the detector angle. The x-ray source is a fine focus copper x-ray tube. The wavelength, λ , of the x-rays is 1.54 Å. The incident beam is conditioned with a four-bounce germanium monochromator. Before the detector, the reflected beam is further conditioned with a three-bounce germanium channel cut crystal. With this configuration, reflectivity fringes (constructive and destructive interference from the film surface and the substrate surface) can be observed from films up to 1.2 μm thick.

The x-ray reflectivity data are fit using a nonlinear least squares algorithm using the recursive multi-layer method.⁹ Model profiles are generated and separated in several layers with varying thickness and electron density, then the resulting reflectivity profiles are calculated. The best fit electron density depth profile to the data provides the overall film thickness, the film roughness, and the average electron density of the film.

Small-angle Neutron Scattering

The small-angle neutron scattering measurements (SANS) are performed on the 8 m NG1 line at the National Institute of Standards and Technology (NIST) Center for Neutron Research. The neutron wavelength, λ , was 6 Å with a wavelength spread $\Delta\lambda/\lambda$ of 0.14. The sample to detector distance was 3.6 m and the detector was offset by 3.5° from the incident beam to increase the range of observable angles. The films were placed so that the film surface is perpendicular to the incident beam. The samples are held in rectangular quartz cells with a 5 mm path length. To increase the scattered intensity from these thin films, up to 6 sample pieces are stacked within the cell. Two-dimensional scattering patterns were collected from the sample for up to five hours for sufficient count statistics. The two-dimensional data were then corrected for empty beam and background scattering using standard reduction methods. The scattered intensity was placed on an absolute intensity scale with reference to a secondary water standard.

Scattering measurements were performed under ambient conditions to determine the structural characteristics of the pore structure. Measurements were also made on samples immersed in deuterated toluene, a solvent that readily wets the sample. Changes in the scattered intensity after immersion provides a measure of the percentage of pores that are interconnected and accessible to the film surface. The scattering data are analyzed using a simple random two-phase description of the film, the Debye model.¹⁰ In this framework, the density of the wall material is assumed to be uniform and the density correlation function describing the film is assumed to be exponential.

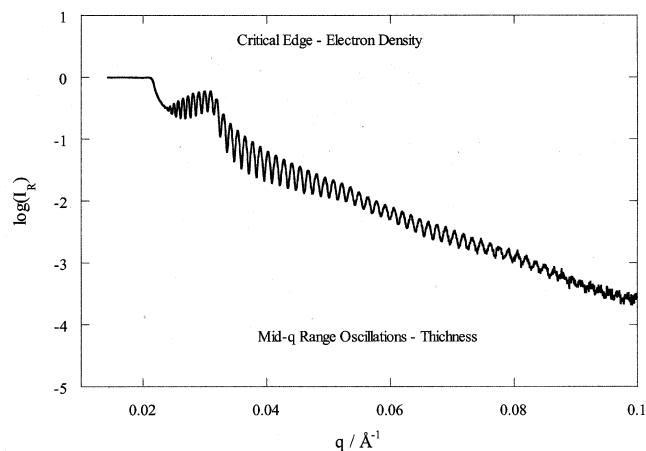


Fig. 1. Typical SXR data showing characteristic critical edge and mid-q range oscillations.

Data Analysis

As an example, we present data and results from a porous silica thin film prepared from a methyl silsesquioxane (MSSQ) spin-on glass resin processed with a porogen material. The porogen material forms domains in the film that are subsequently burned off to form a porous structure. Four samples will be discussed and designated S1, S2, S3, and S4 with increasing amounts of porosity. These samples are not unique in structure, but are simply typical examples of films that have been characterized at NIST. Samples that are best for characterization by this technique have pores that are >10 Å in size and make up a fraction $>5\%$ of the volume of the sample.

The ion scattering experiments provide information on the relative content of the atoms commonly found in thin films, hydrogen, carbon, oxygen, and silicon. This information is necessary to calculate the relative contrast factors for x-ray or neutrons. For example, the reflectivity results give an average electron density of the film. With knowledge of the relative atomic content, the mass density of the film can be calculated. Similarly, the small-angle neutron scattering (SANS) scattering results can give mass density values using a contrast factor that is based on the interaction of neutrons with the individual atoms. Ion scattering also gives values of the total number of atoms on the surface that can be compared to values calculated from reflectivity data.

High-resolution specular x-ray reflectivity (SXR) is a powerful experimental technique to accurately measure the structure of thin films in the direction normal to the film surface. In particular, the film thickness, film quality (roughness and uniformity) and average film density can be determined with a high degree of precision. The coefficient of thermal expansion (CTE) is determined from measurements of the film thickness at different temperatures.

Figure 1 shows (SXR) results from a typical film. The q value at which the film goes from total reflectance to penetration is known as the critical edge. It can be used to calculate the electron density of the

Table I. Atomic Composition and Atomic Film Density from RBS and FRES, Uncertainties are Described in the Data Analysis Section

Sample	Hydrogen	Carbon	Oxygen	Silicon	Atomic Density / (10^{18} atoms/cm 2)
S1	0.28 ± 0.05	0.14 ± 0.05	0.36 ± 0.05	0.22 ± 0.05	1.98 ± 0.05
S2	0.31	0.14	0.35	0.20	1.75 ± 0.04
S3	0.32	0.14	0.34	0.20	1.59 ± 0.04
S4	0.30	0.16	0.34	0.20	0.87 ± 0.02

film. Given the elemental composition, the average electron density of the porous thin film can be converted into an average mass density of the film. The average mass density of the film is also related to the porosity and wall density of the film through the equation

$$\rho_{\text{eff}} = \rho_w(1 - P) \quad (1)$$

where ρ_w is the density of the wall material and P is the porosity of the film (by volume). At this point, an assumption of the matrix mass density can provide a numerical estimate of the film porosity. However, no information about the pore size can be obtained using (SXR). The scattered intensity is presented as a function of q [where $q = (4\pi/\lambda \sin(\theta/2))$ and q is the scattering angle).

In addition to the average mass density of the film, the film thickness can be determined from a more detailed analysis of the reflectivity data or the periodicity of the oscillations in the reflectivity profile. The oscillations at larger angles result from the destructive and constructive interference of the x-rays reflected from both the air/film interface and the film/silicon interface. The thickness of the film can be determined from the periodicity of the reflectivity data in this q range. The oscillations in the reflectivity curve are generally free of multiple scattering contributions. A Fourier transform of the higher angle data enables a model free determination of the film thickness.

With the SANS data, the two-phase model is used to describe a high porosity material. In this model, there are only two phases, the pores and the matrix material. Additionally, the matrix material is assumed to be homogenous. Debye developed the formalism describing the scattering that arises from a random two-phase structure.¹⁰ The density correlation function describing the structure is assumed to be $\gamma(r) = \exp(-r/\xi)$, where ξ is the correlation length. The function $\gamma(r)$ describes the probability that the atomic density at points spaced a distance r apart are the same. The average chord length of the pores is then given by the equation $l_c = \xi/(1-P)$. The SANS intensity is given by the equation

$$I(q) = \frac{8\pi P(1-P)\Delta\rho_n^2 \xi^3}{(1+q^2\xi^2)^2} \quad (2)$$

where $\Delta\rho_n$ is the neutron scattering contrast and is determined by the elemental composition of the solid matrix material and is linearly dependent upon ρ_w .

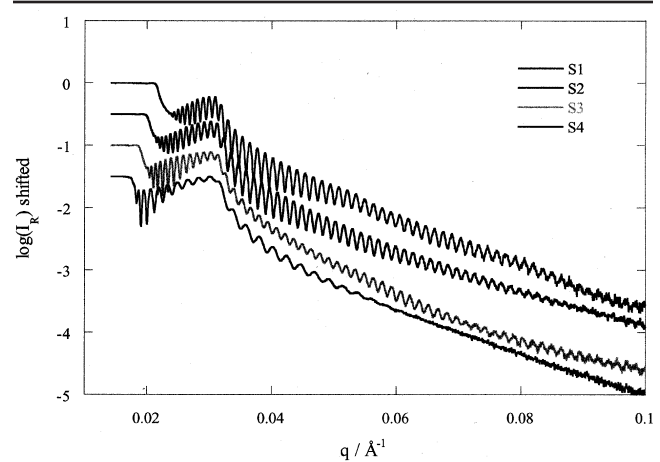


Fig. 2. SXR results of samples S1, S2, S3, and S4 shifted for clarity.

The correlation length, ξ , and the scattered intensity at $q = 0$, can be determined by linearly fitting SANS data plotted as $1/I^{1/2}$ vs. q^2 . At this point in the analysis, only the correlation length is quantitatively determined.

To determine the film porosity, P , and the matrix mass density, we must use additional information from SXR. Given $I(0)$ and ξ , Eq. 2 becomes a function only of ρ_w and P . From the SXR formalism, Eq. 1 is also a function of ρ_w and P . With two equations and two unknowns, ρ_w and P , we solve for these two quantities for the porous thin film. The 2-phase model often provides reasonable values for the density of the wall material, but these values do not necessarily imply that the connecting material is indeed homogeneous.

The pore connectivity and moisture uptake of the film can also be determined using the Debye formalism. The samples are placed into quartz cells and immersed in either deuterated toluene (d-toluene) or deuterated water (D_2O). The d-toluene solvent is chosen because it readily wets most samples. If either of the deuterated solvents penetrates open and interconnected pores, the absolute value of the scattered intensity changes because of the large contrast change in $\Delta\rho_n^2$ from air or vacuum in the pores to a deuterated material. If all the pores within a sample were filled with d-toluene, the entire scattered intensity would increase by a factor of ~ 20 depending on the composition and wall density. If the increase in scattered intensity is less than the predicted value, then only a fraction of the pores are filled with the solvent. In a similar manner, the moisture uptake of D_2O may also

Table II. Thickness, Electron Density, and Mass Density from SXR and Mass Density from RBS and FRES, Uncertainties are Described in the Data Analysis Section

Sample	Thickness/Å	Electron Density / e-Å ⁻³	Mass Density SXR / g cm ⁻³	Mass Density RBS-FRES/g cm ⁻³
S1	4490 ± 10	0.332 ± 0.007	1.082 ± 0.023	1.016 ± 0.026
S2	4510	0.289	0.939	0.850 ± 0.022
S3	4040	0.257	0.833	0.852 ± 0.022
S4	2780	0.224	0.727	0.689 ± 0.018

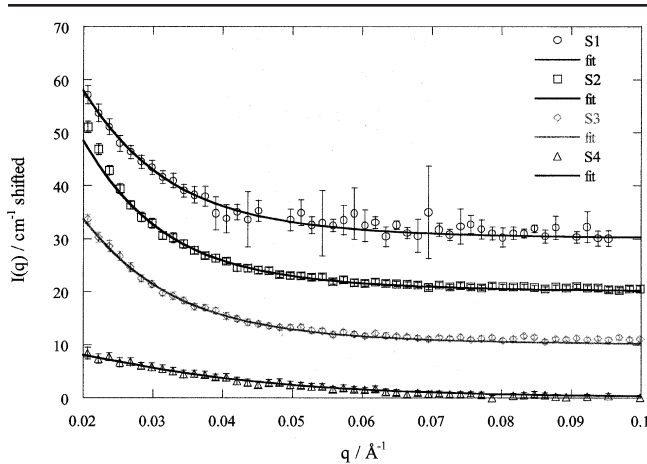


Fig. 3. SANS results of samples S1, S2, S3, and S4 shifted for clarity.

be determined. In this methodology, pore connectivity represents the fraction of pores that are interconnected and accessible to a solvent at the outside surface. Equation 3 gives the calculation of volume fraction of connected pores, P , as a function of SANS intensities in toluene and air, $I_t(q)$ and $I_a(q)$, with contrast factors of toluene and the wall, σ_t and σ_w .

$$\Phi = \frac{(I_t(q)) / (I_a(q)) - 1}{(\sigma_t / \sigma_w - 1)^2 - 1} \quad (3)$$

The primary sources of uncertainties are the statistical scatter in the SANS and reflectivity results, the elemental composition of the film, and the scattering model in the SANS data fit. The Debye fit of the SANS data gives slope, intercept, and their associated standard deviations. These uncertainties are propagated to the zero angle scattering and correlation length. The fit of the reflectivity data gives the thickness and critical angle. The fractional uncertainty of 0.025 for the angle and a relative uncertainty of 10 Å in the

thickness are used for all calculations. The values of the neutron and x-ray contrast factors are calculated from the atomic composition from ion scattering and an uncertainty of 5 atoms per 100 total is assumed, which is based on typical results from this technique. The only other uncertainties accounted for are the value of the secondary standard for SANS and the sample transmission. The fractional uncertainties are taken to be 0.05 and 0.10, respectively. All of the uncertainties represent one standard deviation.

RESULTS AND DISCUSSION

Four films will be described as an example of this technique as described in the experimental section. The elemental analysis from FRES and RBS is given in Table I. All films have very similar atomic fractions and therefore very similar x-ray and neutron contrast factors. The atomic density varies from sample to sample with the values decreasing with increased sample numbers. This decrease is a combination of factors of changing film thickness, porosity, and wall density.

Figure 2 is a plot of the SXR results for the four samples with the scattered intensity shifted for clarity. There are three features to be noted. First, the critical edge shifts to lower q as the sample number increases. This means that the electron density, and hence average mass density, is decreasing. Second, in the mid- q region, the periodicity can easily be seen. The spacing is similar for samples S1–S3, but is wider for S4. This means that the film thicknesses are similar with S4 being somewhat thinner. And third, the peak intensity of the oscillations in the mid- q region is lower for S4 and diminished more rapidly with increased q , suggesting that the uniformity of the surface is decreasing.

Table II gives the calculated thickness of the films along with the average electron and mass densities. Mass densities from the RBS-FRES results are also included. The films are all less than 1/2 μm in thick-

Table III. Porosity, Wall Density, Pore Connectivity, and Pore Size from a Combination of RBS, FRES, SXR, and SANS, Uncertainties are Described in the Data Analysis Section

Sample	Porosity	Connectivity	Wall Density SXR-SANS	Pore $\xi/\text{Å}$
S1	0.20 ± 0.07	1.07 ± 0.53	1.351 ± 0.116	27 ± 3
S2	0.26 ± 0.05	0.57 ± 0.25	1.266 ± 0.096	49 ± 4
S3	0.33 ± 0.06	0.55 ± 0.25	1.234 ± 0.114	61 ± 6
S4	0.37 ± 0.07	0.23 ± 0.12	1.155 ± 0.138	62 ± 8

ness with S4 being approximately $2/3$ the thickness of the others. The density of the films drops with the sample number and the results of the two measurement techniques correlate well. The values of the average mass density are lower than that typical of bulk materials, suggesting that voids are present which lower the overall density average.

Figure 3 is a plot of the SANS results from the four samples, shifted for clarity. The lines are fits to Eq. 2. All of the samples fit the Debye model well showing that an exponential correlation function of pore sizes exists. The drop in intensity with q is more gradual for sample S4 which indicates that there is a smaller correlation length and hence, smaller pores.

Table III shows the calculated values of the porosity, wall density, and average pore size of the four samples. The porosity of the samples increases with the sample number and the wall densities decreases. These parameters depend strongly on both SXR and SANS. The correlation length of the pores increases with the sample number. The pore connectivity is also given in Table III. The standard deviations are sizeable in this parameter because the results of two SANS experiments are combined. The results indicate that S1 is fully connected with the other samples having less than fully connected pores.

SUMMARY

The combination of three experimental measurements, ion scattering/specular x-ray reflectivity/small angle neutron scattering, allows for the detailed analysis of thin film samples. The samples are measured in-situ on a silicon substrate and are nondestructive,

with multiple measurements possible on the same sample. Film thickness, average film density, atomic composition, pore volume, pore connectivity, and pore size can be calculated for thin films (between $0.28\ \mu\text{m}$ and $0.45\ \mu\text{m}$) with moderate porosities (volume fraction between 20% and 37%) and mesoscopic sizes (between $27\ \text{\AA}$ and $62\ \text{\AA}$). It should be noted, however, that the limits of size characterization are greater than the examples given in this report.

REFERENCES

1. C. Jin, J.D. Luttmer, D.M. Smith, and T.A. Ramos, *MRS Bull.* 22, 39 (1997).
2. D.W. Gidley, W.E. Frieze, T.L. Dull, A.F. Yee, C.V. Nguyen, and D.Y. Yoon, *Appl. Phys. Lett.* 76, 1282 (2000).
3. F.N. Dultsev and M.H. Baklanov, *Electron. Solid State Lett.* 2, 192 (1999).
4. W.L. Wu, W.E. Wallace, E.K. Lin, G.W. Lynn, C.J. Glinka, E.T. Ryan, and H.M. Ho, *J. Appl. Phys.* 87, 1193 (2000).
5. E.K. Lin, W.L. Wu, C. Jin, and J.T. Wetzel, *Mater. Technol., and Reliability for Adv. Interconnects and Low-k Dielectrics*, ed. K. Maex et al. (Warrendale, PA: MRS, 2000).
6. W.L. Wu, E.K. Lin, C. Jin, and J.T. Wetzel, *Mater. Technol., and Reliability for Adv. Interconnects and Low-k Dielectrics*, ed. K. Maex et al. (Warrendale, PA: MRS, 2000).
7. J.R. Tesmer and M. Nastasi, *Handbook of Modern Ion Beam Materials Analysis* (Pittsburgh, PA: MRS, 1995).
8. Certain commercial equipment and materials are identified in this paper in order to specify adequately the experimental procedure. In no case does such identification imply recommendation by the National Institute of Standards and Technology nor does it imply that the material or equipment identified is necessarily the best available for this purpose.
9. J. Lekner, *Theory of Reflection* (Dordrecht, the Netherlands: Nijhoff, 1987).
10. P. Debye, H.R. Anderson, and H. Brumberger, *J. Appl. Phys.* 28, 679 (1957).